PHYSICAL REVIEW B **92**, 180411(R) (2015)

$Sc_2Ga_2CuO_7$: A possible quantum spin liquid near the percolation threshold

R. Kumar,[1] P. Khuntia,[2,3] D. Sheptyakov,[4] P. G. Freeman,[5,6] H. M. Rønnow,[5,7] B. Koteswararao,[8,1] M. Baenitz,[3] M. Jeong,[5] and A. V. Mahajan[1,*]

[1]*Department of Physics, Indian Institute of Technology Bombay, Powai, Mumbai 400076, India*
[2]*The Ames Laboratory, US Department of Energy, Ames, Iowa 50011, USA*
[3]*Max-Planck Institute for Chemical Physics of Solids, 01187 Dresden, Germany*
[4]*Laboratory for Neutron Scattering and Imaging, Paul Scherrer Institut, 5232 Villigen PSI, Switzerland*
[5]*Laboratory for Quantum Magnetism (LQM), Ecole Polytechnique Federale de Lausanne (EPFL), CH 1015, Switzerland*
[6]*Jeremiah Horrocks Institute for Mathematics, Physics and Astronomy, University of Central Lancashire, Preston PR1 2HE, United Kingdom*
[7]*Neutron Science Laboratory, Institute for Solid State Physics (ISSP), University of Tokyo, Tokai, Ibaraki 319-1106, Japan*
[8]*School of Physics, University of Hyderabad, Hyderabad 500046, India*

(Received 16 June 2015; revised manuscript received 3 November 2015; published 17 November 2015)

$Sc_2Ga_2CuO_7$ (SGCO) crystallizes in a hexagonal structure (space group: $P6_3/mmc$), which can be seen as an alternating stacking of single and double triangular layers. Combining neutron, x-ray, and resonant x-ray diffraction, we establish that the single triangular layers are mainly populated by nonmagnetic Ga^{3+} ions (85% Ga and 15% Cu), while the bilayers have comparable population of Cu^{2+} and Ga^{3+} ions (43% Cu and 57% Ga). Our susceptibility measurements in the temperature range 1.8–400 K give no indication of any spin-freezing or magnetic long-range order (LRO). We infer an effective paramagnetic moment $\mu_{\rm eff} = 1.79 \pm 0.09\,\mu_B$ and a Curie-Weiss temperature $\theta_{\rm CW}$ of about -44 K, suggesting antiferromagnetic interactions between the $Cu^{2+}(S = 1/2)$ ions. Low-temperature neutron powder diffraction data showed no evidence for LRO down to 1.5 K. In our specific heat data as well, no anomalies were found down to 0.35 K, in the field range 0–140 kOe. The magnetic specific heat C_m, exhibits a broad maximum at around 2.5 K followed by a nearly power law $C_m \propto T^{\alpha}$ behavior at lower temperatures, with α increasing from 0.3 to 1.9 as a function of field for fields up to 90 kOe and then remaining at 1.9 for fields up to 140 kOe. Our results point to a disordered ground state in SGCO.

DOI: 10.1103/PhysRevB.92.180411 PACS number(s): 75.10.Jm, 75.10.Kt, 75.40.Cx

Introduction. Geometrically frustrated spin systems are full of surprises and continue to draw attention because of their tendency to host novel ground states [1]. In particular, triangular lattice based geometrically frustrated Mott insulators have gained wide interest because their ground states were envisaged to be based on a resonating valence bond (RVB) picture [2]. Anderson's RVB proposal [2] pertained to the two-dimensional (2D) edge-shared triangular lattice which, however, has a 120° ordered ground state [3–6]. This, in particular, triggered the search for the RVB state (also called the quantum spin liquid QSL state [1]) in geometries such as triangular (anisotropic), kagome (2D), hyperkagome (three dimensional 3D), and pyrochlore (3D). Finally, a QSL state was realized notably in the 2D triangular system κ-$(BEDT\text{-}TTF)_2Cu_2(CN)_3$ [7], the kagome system $ZnCu_3(OH)_6Cl_2$ [8–12], and the hyperkagome system $Na_4Ir_3O_8$ [13,14]. A frustrated geometry and a low value of spin ($S = 1/2$), which enhances quantum fluctuations, help in stabilizing a QSL state [1]. However, even in the 6H-B and 3C phases of $Ba_3NiSb_2O_9$ (Ni^{2+}, $S = 1$) [15], which have 2D edge-shared triangular and 3D edge-shared tetrahedral lattices, respectively, a QSL state has been suggested. Also, the realization of a QSL state for $Ba_3IrTi_2O_9$ [16], containing a diluted triangular lattice, and $Ba_3YIr_2O_9$ (high pressure cubic phase) [17], possibly suggests the importance of further neighbor interactions and/or deviations from the Heisenberg model. Recent experimental/theoretical results suggest that disorder might even drive the QSL state [18,19]. The unconventional nature of its elementary excitations, which result from a chargeless sector of spin-1/2 fermions (commonly known as spinons), also drew interest from theorists and experimentalists [1,20,21]. Spinons are believed to form a Fermi surface in such Mott insulators and a nonvanishing Sommerfeld coefficient (γ) appears to be a generic feature for most of the previously discussed QSL [7,13,15,17].

We have been exploring a variety of spin systems with the objective of finding new QSL especially investigating triangular lattices. Herein, we introduce a $Cu^{2+}(S = 1/2)$ based potential QSL system $Sc_2Ga_2CuO_7$ (SGCO). This system was first reported by Kimizuka *et al.* [22] and the structure type was identified as similar to $Yb_2Fe_3O_7$ [23]. However, no other data have been reported up to now. Here we report a thorough investigation of the structure and magnetic properties of SGCO by synchrotron x-ray diffraction (xrd), neutron diffraction (ND), susceptibility, and specific heat measurements. In the $Yb_2Fe_3O_7$ structure as applied to SGCO, the 4f sites (forming triangular bilayers) are expected to be occupied by Ga and 2b sites (forming single triangular layers) by Cu (see Fig. 1). However, we found a large deviation from this expectation. The Ga and Cu occupancies are not easy to obtain due to their similar scattering lengths for neutron as well as similar atomic scattering factors for xrd. From the xrd (synchrotron) data, where the x-ray energy was tuned to be near the K-absorption edge of Cu, we could reliably estimate the 4f and 2b site occupancies by Ga and Cu. Combined with our magnetization and heat capacity data, this allows us to suggest that the magnetic lattice of SGCO comprises of (i) triangular biplanes, (double layers of triangular bipyramids), of $S = 1/2$ Cu, which are nearly 50% diluted by Ga but give

*mahajan@phy.iitb.ac.in

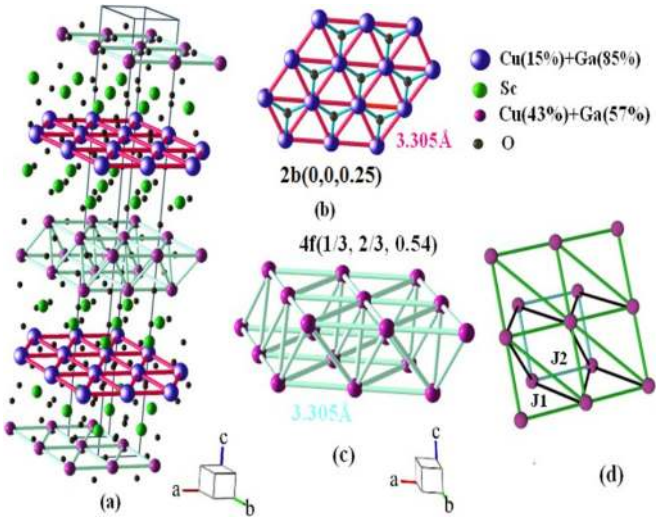

FIG. 1. (Color online) (a) The unit cell of SGCO. (b) Edge-shared triangular plane of the 2b (0, 0, 1/4) sites. (c) Triangular biplanes from the 4f site (1/3, 2/3, 0.54). (d) An alternative representation of (c) (to maintain clarity, not all atoms are shown). The 2b and 4f sites are shared by Cu and Ga (see legend and text).

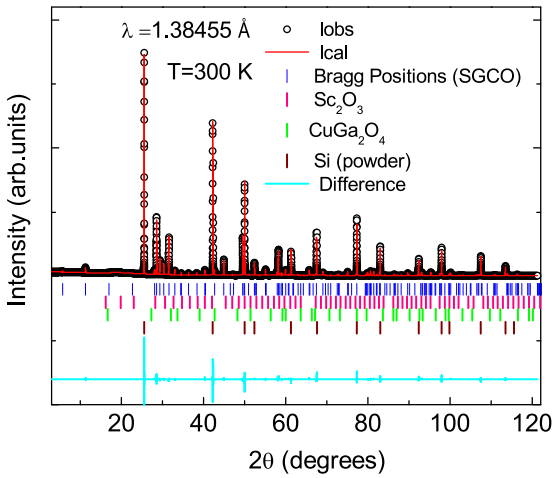

FIG. 2. (Color online) Resonant xrd (SLS) data ($\lambda = 1.38455$ Å) for SGCO at 300 K refined with the space group $P6_3/mmc$. Iobs and Ical represent the experimental and Rietveld refined intensities, respectively. The vertical blue, pink, green and brown bars depict the Bragg positions for SGCO, Sc_2O_3, $CuGa_2O_4$, and Si (internal standard), respectively, whereas the flat cyan line shows Iobs- Ical.

rise to spin liquid behavior and (ii) some uncorrelated Cu located at a different site. For magnetic fields higher than 90 kOe, the magnetic heat capacity exhibits a power law behavior with an exponent close to 2 as in many QSL systems [13,15].

Sample preparation and experimental details. Several batches of polycrystalline SGCO were synthesized by a conventional solid-state reaction route (see Supplemental Material [24]). Xrd data were collected at 300 K using a PANalytical diffractometer using Cu-K_α radiation ($\lambda = 1.54182$ Å). Synchrotron xrd data were measured at room temperature at the Materials Sciences Beamline [25] of the Swiss Light Source (SLS), with the wavelength 0.6204 Å, using the Mythen-II detector. Data were also taken at $\lambda = 1.38455$ Å ($E = 8.9548$ keV), which is just below the K-absorption edge of Cu ($E = 8.9789$ keV). Silicon powder was added to the substance in order to substantially reduce the x-ray absorption in the sample. The ND measurements were carried out with the HRPT diffractometer [26] at the SINQ neutron source ($\lambda = 1.49$ Å) of Paul Scherrer Institut at 300 and 1.5 K using a standard orange cryostat. Magnetization M measurements were done using a Quantum Design SQUID VSM in the temperature T range 1.8–400 K and in magnetic fields H up to 70 kOe. The ac susceptibility measurements were performed on a dilution refrigerator (0.3–7 K) and on a Quantum Design SQUID VSM in the T range 2–30 K [24]. The heat capacity measurements were done in the T-range 0.35–295 K, using a Quantum design PPMS.

Structure and magnetic model. The powder xrd and ND patterns of SGCO could be indexed within the space group $P6_3/mmc$ (194) and correspond to the $Yb_2Fe_3O_7$ structure previously reported by Kimizuka *et al.* [22,23]. Our laboratory xrd data (not shown) did not show any impurity peaks, however, in the much higher statistics synchrotron data we found Sc_2O_3 (∼1.2 wt.%) and $CuGa_2O_4$ (∼0.5 wt.%) impurities. A three-phase Rietveld refinement using FULLPROF [27] was done on our synchrotron data to obtain the lattice constants and the absolute amount of phases. The refined synchrotron data with ($\lambda = 0.62$ Å) and the extracted atomic positions for SGCO are summarized in Ref. [24]. The obtained lattice constants are $a = b = 3.30395(3)$ Å and $c = 28.1116(3)$ Å, similar to those reported by Kimizuka *et al.* [22].

Since Cu and Ga have similar scattering lengths, both for x-rays and for neutrons, possible site sharing between the two is not easily addressed by analyzing the diffraction data. For instance, for x rays ($\lambda = 0.62$ Å), the atomic scattering factors for Ga and Cu are different by only 7%. However, if one tunes the x-ray energy near the K-absorption edge of Cu, the difference in scattering factors for Ga and Cu can be much more. In our case ($\lambda = 1.38455$ Å), the scattering factors for Ga and Cu are different by 25%. Xrd pattern under these conditions is shown in Fig. 2. The obtained lattice constants are $a = b = 3.3045(2)$ Å, $c = 28.1129(1)$ Å (see Ref. [24] for details). We find that the 2b sites (0, 0, 1/4) contain 85% nonmagnetic Ga^{3+} and 15% Cu^{2+}. The 4f sites (1/3,2/3,z) contain 57% $Ga^{3+}$and 43% Cu^{2+} ions. As shown in Fig. 1(b) the edge-shared single-triangular planes at the 2b sites (0, 0, 1/4), along with the neighboring oxygen atoms make single layers of corner-sharing triangular bipyramids (see Ref. [24]). On the other hand, the 4f sites (1/3, 2/3, 0.54) form triangular biplanes [see Fig. 1(c)] or rather double layers of triangular bipyramids when the oxygens are included. In a biplane (4f sites), a triangular layer is shifted with respect to the other such that the vertices of one layer are at the centroids of alternate triangles of the other layer. This is topologically equivalent to a honeycomb lattice with nearest- ($J1$) and next-nearest-neighbor ($J2$) coupling and based on exchange paths it is likely that $J2 > J1$, see Fig. 1(d).

The preference for Ga for the 2b sites is supported by bond-valence sum (BVS) calculations. The BVS for Ga^{3+} is 2.91 on 2b sites and 2.69 on 4f sites, making 2b the preferred site for Ga^{3+}. Likewise, the BVS for Cu is 2.54 on 2b sites and 2.35 on 4f sites, giving a slight preference for Cu^{2+} to occupy 4f sites, in agreement with the results from the structural refinements.

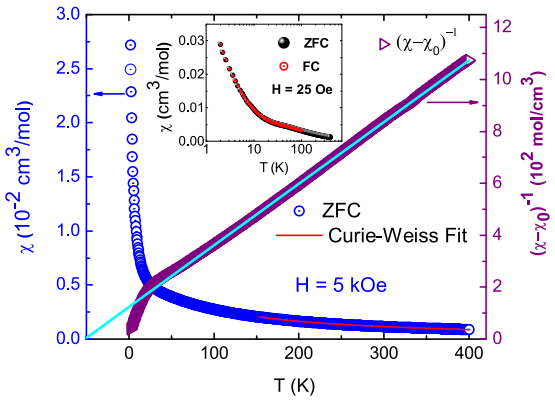

FIG. 3. (Color online) The left y axis shows the T dependence of χ (blue open circles) measured in $H = 5$ kOe and the right y axis shows the inverse χ plot (purple open triangles) free from the T-independent χ. The Curie-Weiss fit is shown in the T-range 150–400 K with a red solid line and the inset depicts the absence of any ZFC/FC bifurcation in $\chi(T)$ in $H = 25$ Oe.

The dc susceptibility ($\chi = \frac{M}{H}$) of SGCO varies in a Curie-Weiss manner $\chi = \chi_0 + C/(T - \theta_{CW})$ down to 100 K, where χ_0 (-4.451×10^{-5} cm^3/mol), $C = 0.41$ cm^3 K/mol, and $\theta_{CW} = -44$ K denote the T-independent χ, the Curie constant, and the Curie-Weiss temperature, respectively. The negative θ_{CW} suggests antiferromagnetic correlations and the inferred effective moment $\mu_{eff} \approx \sqrt{8C} = 1.79 \pm 0.09\ \mu_B$ is close to that for an $S = 1/2$ moment. Measurements performed in a low field (25 Oe) and down to 2 K do not exhibit any anomaly or bifurcation between zero-field-cooled (ZFC) and field-cooled (FC) data (inset of Fig. 3). Alternating current χ_{ac} measurements in the T-range 0.3–30 K do not show any anomaly or frequency dependence (see Ref. [24]). This suggests the absence of LRO or any spin freezing. It is worth mentioning that the ND measurements carried out at 1.5 K did not show any signature of magnetic Bragg peaks, setting an upper limit of 0.5 μ_B for the ordered moment in case of LRO. Further, ^{71}Ga NMR shift data [28] on SGCO indicate a leveling off of χ below about 50 K and the absence of LRO. While further evidence is needed to conclusively establish QSL behavior in SGCO, the essential features of $\chi(T)$ in SGCO are as in other QSL materials.

To estimate the fraction of paramagnetic spins in SGCO, we have made use of the data from magnetic isotherms $M(H)$ at low-T (1.8–4.5 K) since the Cu at the 2b sites is expected to show paramagnetic Curie-like behavior while the contribution from the possibly correlated triangular biplanes might be much lower. Our analysis (see Ref. [24]) of the $M(H)$ data is consistent with about 12% of paramagnetic $Cu^{2+}(S = 1/2)$ spins, which is not far from the value of 15% Cu at the 2b sites obtained from resonant xrd data. In $In_2Ga_2CuO_7$, structurally similar to SGCO, Taetz *et al.* [29] obtained approximately 10% of paramagnetic $S = 1/2$ impurities from a similar analysis. Given the site occupancies obtained from resonant xrd results on SGCO, the magnetic lattice [bilayers from the atoms at 4f positions (1/3, 2/3, 0.54)] is more than 50% diluted. While this is beyond the percolation threshold of a 2D triangular lattice, for the bilayer configuration (or the honeycomb lattice as mentioned before) here, the magnetic connectivity might still be maintained.

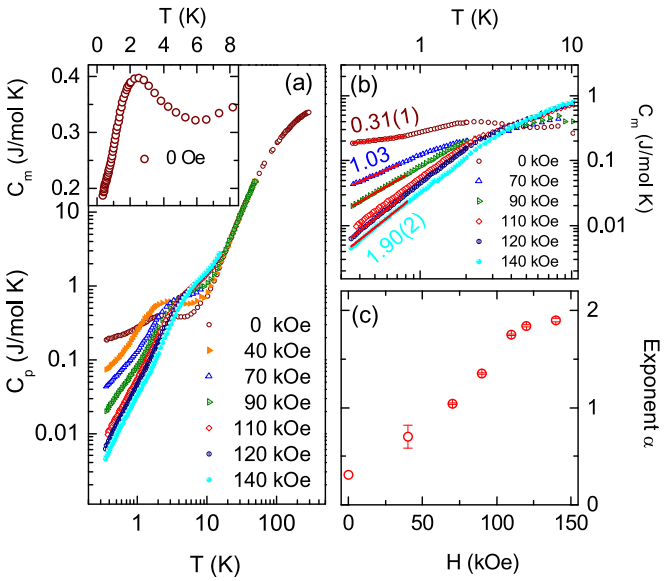

FIG. 4. (Color online) (a) The $C_p(T)$ data (log-log scale) for various H (up to 140 kOe) are shown. Inset depicts the appearance of a broad maximum in C_m, in $H = 0$. (b) Power law fits (see text) of C_m are shown as solid lines. (c) Variation of exponent α with H is shown. Note that for $H > 40$ kOe, the size of the error bars is equal to the size of the symbols.

Based on our experiments, we suggest that SGCO appears to consist of (i) 10%–15% of the 2b sites having $S = 1/2$ paramagnetic moments and (ii) a nearly equal mixture of $S = 1/2$ Cu^{2+} and $S = 0$ Ga^{3+} at the 4f sites, which magnetically form the triangular biplanes. While it could be that the site occupation is correlated, maintaining the magnetic connectivity in the triangular bilayers, it is surprising that there is no spin-freezing even after large dilution. One may speculate that the proximity of the site occupation to a percolation threshold may promote long range spin singlets as in an algebraic spin liquid [1].

Heat capacity. To obtain further insight into the low-energy excitations of SGCO, we measured its specific heat $C_p(T)$ (Fig. 4) in the T-range 0.35–300 K under various H (0–140 kOe). We found no signature of LRO down to 0.35 K. However, below about 15 K the $C_p(T)$ displays a dependence on H which is suggestive of a Schottky anomaly. This Schottky contribution $C_{Schottky}$ most likely arises from the paramagnetic Cu^{2+} spins at the 2b sites. Note that our $M(H)$ data analysis revealed a ~12% contribution from paramagnetic $S = 1/2$ species. We then analyzed $C_p(T)$ as a combination of $C_{Schottky}$ and $C_{lattice}$ (the lattice heat capacity) in addition to a magnetic heat capacity C_m (see Ref. [24]). The C_m (which, we believe, comes from the correlated spins of the triangular biplanes) is obtained after subtracting $C_{lattice}$ and $C_{Schottky}$ and is shown in Fig. 4(b).

As shown in the inset of Fig. 4(a), $C_m(T)$ shows a broad maximum (perhaps not related to any phase transition) at around 2.5 K in $H = 0$. The appearance of a broad maximum is common for highly frustrated spin systems and has previously been noticed for $NiGa_2S_4$ [30], $Na_4Ir_3O_8$ [13], $Ba_3CuSb_2O_9$ [31], and $Ba_3NiSb_2O_9$ [15]. However, its position in T (in

comparison to the strength of the exchange coupling) varies from material to material.

Finally, the low-T C_m data ($T < 1$ K) were fitted to a power-law $C_m = \gamma T^{\alpha}$(where γ is a constant), to infer about the magnetic excitations [see Fig. 4(b)]. We found that in SGCO, α increases from 0.3 to 1.9 with increasing H. The error bars for α in Fig. 4(c) were arrived at by assuming a $\pm 50\%$ uncertainty in C_{Schottky}. The value of α is robust and reliable for $H > 40$ kOe in the T-range 0.35–1 K, and attains a value 1.9(2) for $H > 90$ kOe. An exponent close to 2 might be an indication of a QSL and has previously been observed for the hyperkagomé compound $Na_4Ir_3O_8$ [13] as also the 3C phase of $Ba_3NiSb_2O_9$ [15]. In the case of a kagome lattice, a theoretical approach (spin-1/2 spinons obeying the Dirac spectrum [32]) leads to a T^2 dependence of specific heat. However, there could be other explanations. Recently, randomness-induced QSL (also called random singlet) has been suggested for organic triangular salts [33] as also for inorganic ones such as herbertsmithite [34] with the kagome structure. In herbertsmithite, a Zn/Cu disorder might cause a random Jahn-Teller distortion of the $[Cu(OH)_6]^{4-}$ giving rise to a random modification of the exchange coupling in the kagome layer. For the resulting gapless QSL state, a T-linear C_m is expected. In the SGCO case, a similar Ga/Cu disorder exists which might drive the QSL state. However, In SGCO (in zero field), the power law exponent of C_m is 0.3. This amounts to a divergence of C_m/T at low T. Such a divergence in $Pr_2Ir_2O_7$ (frustrated moments in a metallic background; different than SGCO) has been seen as an indication of proximity to a quantum critical point QCP [35]. For SGCO, with the increasing $C_m(T)$ exponent (from 0.3 to 1.9) with field, one might speculate that the system moves from a QCP to deeper into the insulating QSL region with field. A cautionary note is that the inferred low-field C_m might be affected by possible interaction between the correlated spins and the orphan spins.

It is worth mentioning that in our C_m data at $H = 140$ kOe, $\gamma \sim 34$ mJ/mol $K^{2.9}$. A nonzero value of γ, in general, indicates the presence of low-energy (likely) gapless excitations for these Mott insulators at low T. While the reason for the field-induced suppression of the C_m (suggesting a suppression of magnetic excitations) is not clear at this point, it could arise from a freezing out of any interaction between the orphan spins (Cu^{2+} in the 2b sites) and the triangular bilayers. The estimated entropy change ΔS (see Ref. [24]) by integrating the C_m/T versus T data (in zero field) yields 1.2 J/mol K, which is nearly 20% of that expected for a $S = 1/2$ moment. This value will be even smaller when the data at the highest field are considered. The significantly smaller ΔS is suggestive of a large residual entropy at low temperatures, further suggesting a QSL ground state in SGCO.

Summary. Using the results obtained from various experimental probes such as xrd, ND, dc/ac $\chi(T)$, $M(H)$, and $C_p(T)$, we have explored the properties of SGCO. Our resonant xrd measurements carried out at the K-absorption edge of Cu allow us to infer the site occupancies of Cu and Ga at the 2b sites (Cu:Ga = 0.15:0.85) and the 4f sites (Cu:Ga = 0.43:0.57). We suggest that the magnetic lattice can be viewed as a combination of (i) highly depleted triangular bilayers (or honeycomb layers with nearest- as also next-nearest-neighbor interactions) giving rise to correlated behavior and (ii) about 15% Cu spins which are paramagnetic. Our ND data down to 1.5 K do not show any signature of LRO/spin freezing and are consistent with the dc/ac $\chi(T)$ measurements. Further, the $C_p(T)$ data indicate absence of any transition down to 0.35 K. They are also indicative of the presence of low-energy excitations and for high fields yield $C_m \propto T^2$ below 1 K. Taken together, the apparent lack of LRO or spin freezing and the existence of low-energy (likely gapless) excitations could be indicative of a QSL ground state. Often QSL candidates with site-disorder have been found to display spin freezing. It is therefore unusual to find the combined lack of order and spin-freezing in a system so heavily diluted as the triangular bilayers are in this compound. This could be a result of the dilution approaching a percolation threshold and one may speculate if the unusual QSL behavior could arise close to such thresholds. There is also recent work [19] that proposes disorder driven spin-orbital liquid in such systems. Another possibility is disorder induced bond randomness, which can give rise to a random singlet QSL as has been suggested in herbertsmithite [34]. Further low-T magnetization and local probe investigations such as μSR would be useful to explore the properties of SGCO in greater details.

Acknowledgments. We thank Department of Science and Technology, Government of India and the Indo-Swiss joint research programme, the Swiss National Science Foundation and its SINERGIA network MPBH for financial support. R. Kumar acknowledges CSIR (India) for awarding him a research fellowship, and B. Koteswararao thanks DST (India) INSPIRE fellowship to carry out the research work. This work is partly based on experiments performed at the Swiss spallation neutron source SINQ, Paul Scherrer Institute, Villigen, Switzerland.

[1] L. Balents, Nature (London) **464**, 199 (2010).
[2] P. W. Anderson, Mater. Res. Bull. **8**, 153 (1973).
[3] B. Bernu, P. Lecheminant, C. Lhuillier, and L. Pierre, Phys. Rev. B **50**, 10048 (1994).
[4] R. R. P. Singh and D. A. Huse, Phys. Rev. Lett. **68**, 1766 (1992).
[5] D. J. J. Farnell, R. F. Bishop, and K. A. Gernoth, Phys. Rev. B **63**, 220402(R) (2001).
[6] L. Capriotti, A. E. Trumper, and S. Sorella, Phys. Rev. Lett. **82**, 3899 (1999).
[7] Y. Shimizu, K. Miyagawa, K. Kanoda, M. Maesato, and G. Saito, Phys. Rev. Lett. **91**, 107001 (2003).
[8] J. S. Helton, K. Matan, M. P. Shores, E. A. Nytko, B. M. Bartlett, Y. Yoshida, Y. Takano, A. Suslov, Y. Qiu, J.-H. Chung, D. G. Nocera, and Y. S. Lee, Phys. Rev. Lett. **98**, 107204 (2007).
[9] P. Mendels, F. Bert, M. A. de Vries, A. Olariu, A. Harrison, F. Duc, J. C. Trombe, J. S. Lord, A. Amato, and C. Baines, Phys. Rev. Lett. **98**, 077204 (2007).
[10] T. Imai, E. A. Nytko, B. M. Bartlett, M. P. Shores, and D. G. Nocera, Phys. Rev. Lett. **100**, 077203 (2008).

[11] A. Olariu, P. Mendels, F. Bert, F. Duc, J. C. Trombe, M. A. de Vries, and A. Harrison, Phys. Rev. Lett. **100**, 087202 (2008).
[12] M. A. de Vries, J. R. Stewart, P. P. Deen, J. Piatek, G. N. Nilsen, H. M. Ronnow, and A. Harrison, Phys. Rev. Lett. **103**, 237201 (2009).
[13] Y. Okamoto, M. Nohara, H. Aruga-Katori, and H. Takagi, Phys. Rev. Lett. **99**, 137207 (2007).
[14] Y. Singh, Y. Tokiwa, J. Dong, and P. Gegenwart, Phys. Rev. B **88**, 220413(R) (2013).
[15] J. G. Cheng, G. Li, L. Balicas, J. S. Zhou, J. B. Goodenough, Cenke Xu, and H. D. Zhou, Phys. Rev. Lett. **107**, 197204 (2011).
[16] Tusharkanti Dey, A. V. Mahajan, P. Khuntia, M. Baenitz, B. Koteswararao, and F. C. Chou, Phys. Rev. B **86**, 140405(R) (2012).
[17] Tusharkanti Dey, A. V. Mahajan, R. Kumar, B. Koteswararao, F. C. Chou, A. A. Omrani, and H. M. Ronnow, Phys. Rev. B **88**, 134425 (2013).
[18] T. Furukawa, K. Miyagawa, T. Itou, M. Ito, H. Taniguchi, M. Saito, S. Iguchi, T. Sasaki, and K. Kanoda, Phys. Rev. Lett. **115**, 077001 (2015).
[19] A. Smerald and F. Mila, Phys. Rev. Lett. **115**, 147202 (2015).
[20] X. G Wen, Phys. Rev. B **65**, 165113 (2002).
[21] T. K. Ng and P. A. Lee, Phys. Rev. Lett. **99**, 156402 (2007).
[22] N. Kimizuka and T. Mohri, J. Solid State Chem. **60**, 382 (1985).
[23] N. Kimizuka, A. Takenaka, Y. Sasada, and T. Katsura, Solid State Comm. **15**, 1199 (1974).
[24] See Supplemental Material at http://link.aps.org/supplemental/10.1103/PhysRevB.92.180411 for sample preparation, x-ray, neutron refinement, magnetic, and specific heat analysis.
[25] http://www.psi.ch/sls/ms/powder-diffraction.
[26] P. Fischer, G. Frey, M. Koch, M. Könnecke, V. Pomjakushin, J. Schefer, R. Thut, N. Schlumpf, R. Bürge, U. Greuter, S. Bondt, and E. Berruyer, Physica B **276–278**, 146 (2000).
[27] J. Rodríguez-Carvajal, Physica B **192**, 55 (1993).
[28] P. Khuntia *et al.* (unpublished).
[29] T. Taetz, Ph.D. thesis, University of Cologne, Germany, 2008.
[30] S. Nakatsuji, Y. Nambu, H. Tonomura, O. Sakai, S. Jonas, C. Broholm, H. Tsunetsugu, Y. Qiu, and Y. Maeno, Science **309**, 1697 (2005).
[31] H. D. Zhou, E. S. Choi, G. Li, L. Balicas, C. R. Wiebe, Y. Qiu, J. R. D. Copley, and J. S. Gardner, Phys. Rev. Lett. **106**, 147204 (2011).
[32] Y. Ran, M. Hermele, P. A. Lee, and X.-G. Wen, Phys. Rev. Lett. **98**, 117205 (2007).
[33] K. Watanabe, H. Kawamura, H. Nakano, and T. Sakai, J. Phys. Soc. Japan **83**, 034714 (2014).
[34] T. Shimokawa, K. Watanabe, and H. Kawamura, Phys. Rev. B **92**, 134407 (2015).
[35] Y. Tokiwa, J. J. Ishikawa, S. Nakatsuji, and P. Gegenwart, Nat. Mater. **13**, 356 (2014).